HEAT AND MASS TRANSFER IN 3-D MHD WILLIAMSON-CASSON FLUIDS FLOW OVER A STRETCHING SURFACE WITH NON-UNIFORM HEAT SOURCE/SINK

by

Chakravarthula S. K. RAJU[a], Naramgari SANDEEP[b], Mohamed E. ALI[c*], and Abdullah O. NUHAIT[c]

[a] Department of Mathematics, Gitam University, Bengaluru, Karnataka, India
[b] Department of Mathematics, Central University of Karnataka, Kalaburagi, India
[c] Mechanical Engineering Department, College of Engineering, King Saud University, Riyadh, Saudi Arabia

Original scientific paper
https://doi.org/10.2298/TSCI160426107R

A mathematical model has been proposed for investigating the flow, heat, and mass transfer in Williamson and Casson fluid-flow over a stretching surface. For controlling the temperature and concentration fields we considered the space and temperature dependent heat source/sink and homogeneous-heterogeneous reactions, respectively. Numerical results are carried out for this study by using Runge-Kutta based shooting technique. The effects of governing parameters on the flow, heat and mass transfer are illustrated graphically. Also computed the skin-friction coefficients for axial and transverse directions along with the local Nusselt number. In most of the studies, homogeneous-heterogeneous profiles were reduced into a single concentration equation by assuming equal diffusion coefficients. For the physical relevance, without any assumptions we studied the individual behavior of the homogeneous-heterogeneous profiles. It is found that the rate of heat and mass transfer in Casson fluid is significantly large while equated with the heat and mass transfer rate of Williamson fluid.

Key words: *MHD, non-Newtonian fluid, non-uniform heat source/sink, stretching sheet, homogeneous-heterogeneous reactions*

Introduction

The boundary-layer flow, heat and mass transfer over a stretching surface has benefitted believed attention due to its demand in the industrial and manufacturing processes. Such demanded applications are of polymer, chemical industries, controlling of cooling and heating processes, and blood flows. Due to this significance the innovation of the boundary-layer flow past a stretching sheet was initiated by Sakiadis [1]. The study of flow through stretching sheet in the presence of chemical reaction place an important role in the chemical engineering, biomedical, pharmaceutical industries, polythene paper production, and environmental engineering processes these were given by Ali and Al-Yousef [2]. Later on, the self-similarity solution of continuously stretched surfaces with decreasing velocities was discussed by Magyari *et al.* [3]. An analytical solution for MHD flow past a permeable vertical stretching surface with existing of chemical reaction was discussed by Chamka [4]. Raptis and Perdikis [5] analyzed the MHD

* Corresponding author, e-mail: mali@ksu.edu.sa

2-D viscous flow through a non-linearly stretching sheet with existing of chemical reaction. The chemical reaction and heat generation effect on the flow through porous medium was illustrated by Patil and Kulkarni [6]. Mixed convection on flow over a moving vertical surface in the presence of variable viscosity was analyzed by Ali [7]. The mass transfer analysis of MHD flow of a second grade fluid past a permeable stretching sheet in the presence of chemical reaction was studied by Cortell [8].

Past few decades heat and mass transfer in non-Newtonian fluid-flows are playing a vital role than heat and mass transfer in Newtonian fluids due to its simplicity in nature. There are many practical real time, engineering applications of non-Newtonian fluids such as crystal growing, drilling mud's, gels, shampoos, powder technology, food processing, blood flow, and biological applications. There are various types of non-Newtonian fluids like Casson, visco-elastic, Jeffrey, and Williamson fluid. There is no constitutive relation for these fluids so these fluids have simplicity in nature. In the present study, we considered the Casson fluid, it is a shear thinning liquid having an infinite viscosity at rate of shear stress is zero. Owing to this Raju *et al.* [9] analyzed an unsteady Casson fluid-flow through a stretching sheet in the presence of variable thermal conductivity. Haq *et al.* [10] studied the heat transfer characteristics of a Casson nanofluid-flow past a shrinking sheet. An unsteady Casson fluid-flow past an oscillating vertical plate was studied analytically by Hussain *et al.* [11]. Raju *et al.* [12] investigated the mass transfer analysis of MHD Casson fluid-flow past a permeable exponentially stretching sheet. The Casson fluid-flow past an exponentially shrinking surface was illustrated by Nadeem *et al.* [13]. Most of the aforementioned studies are belonging to 2-D, steady, unsteady, exponentially stretching sheets. The 3-D flow of non-Newtonian fluids through a stretching surface also has most applications in the civil engineering, solar energy, and peristalsis blood flow through a pumps, *etc.* Nadeem *et al.* [14] depicted the 3-D flow of Casson nanofluid through a linear stretching surface. Couple stress fluid-flow through a stretching sheet in the presence of Newtonian heating effect was discussed by Ramezan *et al.* [15]. Hayat *et al.* [16] depicted the radiation effect on 3-D Jeffrey fluid-flow past a stretching surface in the presence of variable thermal conductivity. The natural convection flow induced by a continuous stretched sheets in the presence of rapidly depreciating velocities Ali [17].

The MHD flows with non-uniform heat source/sink also plays major in the fields of aerodynamics, aeronautical engineering, astrophysics, space technology, environmental engineering, *etc*. The Williamson fluid-flow past a stretching sheet also have vital role in the field of plasma dynamics, blood flows, ice slurries, ice creams, paste, oil crude preparation, petroleum engineering sandwich processes, bio thermal engineering, *etc*. In modern technology, the researchers are interested into the Williamson fluid-flow through a stretching sheet due to its applications in blood flows and these were addressed by researchers [18-23]. Hayat *et al.* [24] explored the convective conditions on peristaltic flow with homogeneous-heterogeneous reactions. Homogeneous-heterogeneous reaction effect on stagnation-point flow past a stretching surface was illustrated by Bachok *et al.* [25]. Chatterjee [26] studied the steady axisymmetric Carreau fluid jet flow through an impinging surface. Viscoelastic fluid-flow past a saturated porous medium was analyzed by Delenda *et al.* [27]. The researchers [28-35] analyzed the flow over various geometries (cone, plate and sheet) with various flow physical characteristics (non-uniform heat source or sink, nanoliquids, and magnetic field).

All the aforementioned studies concentrated on 2-D or 3-D flows in the presence of chemical reaction, magnetic field, and radiation. But no studies have been described yet up to the author's knowledge on the flow of 3-D non-Newtonian fluids over a stretching surface in the presence of non-uniform heat source/sink and homogeneous-heterogeneous reactions. By

keeping this into view in this study we make an attempt to analyze the heat and mass transfer behavior of the 3-D Casson and Williamson fluid-flows through a stretching sheet with non-uniform heat source/sink and homogeneous-heterogeneous reactions.

Flow analysis

In this study we consider the electrically conducting Casson and Williamson fluid-flows past a stretching sheet in the presence of magneticfield, non-uniform heat source/sink and homogeneous-heterogeneous reactions. The magnetic Reynolds is negligible in this study. Due to this cause we neglected the induced magnetic field. The mass transport was controlling by homogeneous and heterogeneous reactions. The flow configuration is displayed in fig. 1. The rheological model for an isotropic flow of Casson fluid is given by Raju and Sandeep [36]:

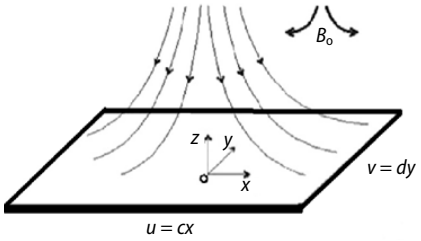

Figure 1. Flow configuration

$$\tau^{1/n} = \tau_0^{1/n} + \mu\dot{\gamma}^{1/n} \tag{1}$$

$$\tau_{i,j} = \begin{cases} 2\left(\mu_B + \dfrac{p_y}{\sqrt{2\pi}}\right)e_{ij}, & \pi > \pi_c \\ 2\left(\mu_B + \dfrac{p_y}{\sqrt{2\pi}}\right)e_{ij}, & \pi < \pi_c \end{cases} \tag{2}$$

where $\pi = e_{ij}e_{ij}$ and e_{ij} is the $(i, j)^{\text{th}}$ component of the deformation rate, π – the product of the component of deformation rate with itself, π_c – a critical value of this product based on the non-Newtonian model, μ_B – the plastic dynamic viscosity of non-Newtonian fluid, and p_y – the yield stress of the fluid. The anonymous researchers has suggested the value of $n = 1$. However, in many applications this value is $n > 1$.

Similarly, the constitutive equation for Williamson fluid model is given by (Nadeem *et al.* [37]):

$$S = -p\vec{\mathrm{I}} + \boldsymbol{\tau} \tag{3}$$

$$\boldsymbol{\tau} = \left[\mu_\infty + \frac{\mu_0 - \mu_\infty}{1 - \Gamma\dot{\gamma}}\right]\boldsymbol{A}_1 \tag{4}$$

Here p is the pressure, $\vec{\mathrm{I}}$ – the identity vector, $\boldsymbol{\tau}$ – the extra stress tensor, μ_0 and μ_∞ are – the limiting viscosities at zero and infinite shear rate, respectively. The $\Gamma > 0$ is the time constant, $\boldsymbol{A}_1$ is the first Rivlin Erickson tensor, and, $\dot{\gamma}$ is defined:

$$\dot{\gamma} = \sqrt{\frac{1}{2\pi}}, \quad \pi = \mathrm{trace}(\boldsymbol{A}_1^2) \tag{5}$$

Here we have only considered the case for which $\mu_\infty = 0$ and $\Gamma\dot{\gamma} < 1$. Thus, extra stress tensor takes the form:

$$\boldsymbol{\tau} = \left[\frac{\mu_0}{1 - \Gamma\dot{\gamma}}\right]\boldsymbol{A}_1 \tag{6}$$

In this study we combined the Casson and Williamson and based on assumptions the governing boundary-layer equations are given by (Haq *et al.* [10], Nadeem *et al.* [13], Raju and Sandeep [36]):

$$\frac{\partial u}{\partial x}+\frac{\partial v}{\partial y}+\frac{\partial w}{\partial z}=0 \tag{7}$$

$$\left(u\frac{\partial u}{\partial x}+v\frac{\partial u}{\partial y}+w\frac{\partial u}{\partial z}\right)=\nu\left(1+\frac{1}{\beta}\right)\frac{\partial^2 u}{\partial z^2}-\frac{\sigma {B_0}^2}{\rho}u+\sqrt{2}\Gamma\frac{\partial u}{\partial z}\frac{\partial^2 u}{\partial z^2} \tag{8}$$

$$\left(u\frac{\partial v}{\partial x}+v\frac{\partial v}{\partial y}+w\frac{\partial v}{\partial z}\right)=\nu\left(1+\frac{1}{\beta}\right)\frac{\partial^2 v}{\partial z^2}-\frac{\sigma {B_0}^2}{\rho}v+\sqrt{2}\Gamma\frac{\partial v}{\partial z}\frac{\partial^2 v}{\partial z^2} \tag{9}$$

The corresponding boundary conditions are:

$$\begin{gathered}u=u_w(x)=cx,\quad v=v_w(y)=dy,\quad w=0,\quad \text{at}\quad z=0\\ u\to 0,\quad v\to 0,\quad w\to 0,\quad \text{at}\quad z=\infty\end{gathered} \tag{10}$$

In the previous equations $\beta\to\infty$, $\Gamma\neq 0$ is called Williamson fluid and $\beta\neq 0$, $\Gamma=0$ is called Casson fluid. To convert the governing equations into set of non-linear ODE, we now introduce the following similarity transformation:

$$u=cxf'(\eta),\quad v=dyg'(\eta),\quad w=-(c\nu)^{0.5}[f(\eta)+g(\eta)],\quad \eta=\upsilon_f{}^{-0.5}c^{0.5}z \tag{11}$$

The eqs. (4) and (5) are substitute into eqs. (1)-(3) we get newly coupled transformed non-linear equation, which are given:

$$\left(1+\frac{1}{\beta}\right)f'''+\lambda f'f'''-Mf'+(f+g)f''-f'^2=0 \tag{12}$$

$$\left(1+\frac{1}{\beta}\right)g'''+\lambda g'g'''-Mg'+(f+g)g''-g'^2=0 \tag{13}$$

The transformed boundary conditions are:

$$\begin{gathered}f=0,\quad g=0,\quad f'=1,\quad g'=1,\quad \text{at}\quad \eta=0\\ f'=0,\quad g'=0,\quad \text{at}\quad \eta\to\infty\end{gathered} \tag{14}$$

where β is the Casson parameter, λ – the Non-Newtonian Williamson fluid parameter, M – the magneticfield parameter, and B_o is the strenght of the applied magnetic field which are given:

$$\lambda=\Gamma x\sqrt{\frac{2c^3}{\nu}},\quad M=\frac{\sigma B_0^2}{\rho c}$$

For engineering interest physical quantities are the shear stress coefficients C_{fx}, C_{fy} (friction factors) are given:

$$\mathrm{Re}_x^{1/2}C_{fx}=\left(1+\frac{1}{\beta}\right)\lambda f''(0),\quad \mathrm{Re}_x^{1/2}C_{fy}=\left(1+\frac{1}{\beta}\right)\lambda g''(0) \tag{15}$$

Heat transfer analysis

The energy equation with non-uniform heat source or sink is given:

$$\left(u\frac{\partial T}{\partial x}+v\frac{\partial T}{\partial y}+w\frac{\partial T}{\partial z}\right)=\alpha\frac{\partial^2 T}{\partial z^2}+\frac{1}{\rho c_p}q''' \tag{16}$$

The boundary conditions for the energy equation is given:

$$T=T_w,\quad \text{at}\quad z=0,\quad T=T_\infty,\quad \text{as}\quad z\to\infty \tag{17}$$

The time dependent non-uniform heat source/sink q''' is defined:

$$q'''=\frac{ku_w(x)}{x\nu}\left[A^*(T_\text{w}-T_\infty)f'+B^*(T-T_\infty)\right] \tag{18}$$

in the previous equation positive values of A^*, B^* correspond to heat generation and negative values are correspond to heat absorption. We define a dimensionless parameter for temperature variable $\theta(\eta)$ of the form:

$$\theta(\eta)=\frac{T-T_\infty}{T_\text{w}-T_\infty} \tag{19}$$

Substituting eq. (13) into eqs. (10)-(12) we get the transformed non-dimensional temperature equation as given:

$$\theta''+\text{Pr}(f+g)\theta'+A^*f'+B^*\theta=0 \tag{20}$$

With the transformed boundary conditions:

$$\theta=1,\quad \text{at}\quad \eta=0,\quad \theta=0,\quad \text{as}\quad \eta\to\infty \tag{21}$$

The local Nusselt number is defined:

$$\text{Nu}_x=\frac{xq_w}{k_f(T_\text{w}-T_\infty)}\quad \text{where}\quad q_w=-k\left(\frac{\partial T}{\partial z}\right)_{z=0} \tag{22}$$

$$\text{Re}_x^{-1/2}\,\text{Nu}_x=-\theta'(0) \tag{23}$$

Mass transfer analysis

It is assumed that a simple homogeneous-heterogeneous reaction model exists as proposed by Chaudhary and Merkin [38] in the following form:

$$\left(u\frac{\partial a}{\partial x}+v\frac{\partial a}{\partial y}+w\frac{\partial a}{\partial z}\right)=D_A\frac{\partial^2 a}{\partial z^2}-k_c ab^2 \tag{24}$$

$$\left(u\frac{\partial b}{\partial x}+v\frac{\partial b}{\partial y}+w\frac{\partial b}{\partial z}\right)=D_B\frac{\partial^2 b}{\partial z^2}+k_c ab^2 \tag{25}$$

The respective boundary conditions are given:

$$\begin{aligned} &D_A\frac{\partial a}{\partial z}=k_s a(z),\quad D_B\frac{\partial b}{\partial z}=-k_s a(z)\quad \text{at}\quad z=0\\ &a(z)=a_0,\quad b(z)=0\qquad\qquad\qquad\qquad \text{as}\quad z\to\infty \end{aligned} \tag{26}$$

where *a, b* are the concentrations of the chemical species, D_A and D_B are the diffusion coefficients, k_c and k_s are the rate constants. We now introduced the similarity transformations:

$$G(\eta)=\frac{a}{a_0},\quad H(\eta)=\frac{b}{a_0} \tag{27}$$

By substituting eq. (21) into eqs. (18) and (19) we get:

$$G"+\mathrm{Sc}[(f+g)G'-KGH^2]=0 \tag{28}$$

$$\delta H''+\mathrm{Sc}[(f+g)H'+KGH^2]=0 \tag{29}$$

The transformed boundary conditions are:

$$\begin{aligned} &G'=K_sG,\quad \delta H'=-K_sG \quad \text{at} \quad \eta=0\\ &G=1,\quad H=0 \qquad\qquad\quad \text{as} \quad \eta\to\infty \end{aligned} \tag{30}$$

whrere Sc is the Schmidt number, K – the measure of strength of homogeneous reaction, K_s – the strength of heterogeneous reaction, $\mathrm{Re}=c/\nu$ – the Reynolds number, and δ is the ratio of diffusion coefficients, which are represented:

$$\delta=\frac{D_B}{D_A},\quad \mathrm{Sc}=\frac{\nu}{D_A},\quad K=\frac{k_c{a_0}^2}{c},\quad K_s=\frac{k_s}{D_A\sqrt{\mathrm{Re}}} \tag{31}$$

For physical quantities of engineering interest the local Sherwood number Sh_x is given:

$$\mathrm{Re}_x^{-1/2}\,\mathrm{Sh}_x=-\phi'(0) \tag{32}$$

Method of solution

To solve the present problem, eqs. (6), (7), (14), (22), and (23) with the corresponding boundary conditions, eqs. (8), (15) and (24), are transformed into a set of first order differential equations. Now, Runge-Kutta and Shooting technique is applied to develop the numerical code. In this methodology, the aforementioned non-linear ODE converted to a first order differential equation, by using the following method:

$$\begin{gathered} f'=y2,\quad f"=y3,\quad g'=y5,\quad g''=y6,\quad \theta=y7,\quad \theta'=y8,\\ G=y9,\quad G'=y10,\quad H=y11,\quad H'=y12 \end{gathered} \tag{33}$$

$$f'''=\frac{1}{\left(1+\lambda y2+\dfrac{1}{\beta}\right)}\left[My2+(y1+y4)y3-y2^2\right] \tag{34}$$

$$g'''=\frac{1}{\left(1+\lambda y2+\dfrac{1}{\beta}\right)}\left[My5+(y1+y4)y5-y5^2\right] \tag{35}$$

$$\theta''=-\mathrm{Pr}[(y1+y4)y8]-A^*y2-B^*y7 \tag{36}$$

$$G''=-\mathrm{Sc}[(y1+y4)y10+Ky9y11^2] \tag{37}$$

$$H''=-\mathrm{Sc}[(y1+y4)y12+Ky9y11^2] \tag{38}$$

with boundary conditions are:

$$\begin{gathered} y1=0,\quad y2=1,\quad y4=0,\quad y5=1,\quad y7=1,\quad y10=K_s y9,\quad \delta y12=-K_s y9 \quad \text{at} \quad \eta\to 0 \\ y2=0,\quad y5=0,\quad y7=0,\quad y9=1,\quad y11=0 \quad \text{at} \quad \eta\to\infty \end{gathered} \tag{39}$$

Initially, the guess values of $y3(0)$, $y6(0)$, $y8(0)$, are used in the simulation which are not given at the initial condition. In this study, the successive iteration length is 0.01. Firstly, the accuracy of the guess values $y3(0), y6(0), y8(0)$ is verified by comparing the estimated values of $y2(0), y4(0), y5(0), y7(0)$ at $\eta=\eta_{\max}$ using MATLAB software ode45 solver. Finally, the Runge-Kutta fourth order method is used to integrate the eqs. (28)-(32) and the iteration continued until the agreement between the estimated values and given condition at $\eta=\eta_{\max}$. It is found that a grid size of 300 ensure the grid independent solution for the present case. The accuracy of the present numerical simulation results are validated with the previous study of Ahmad and Nazar [39], see, tab. 3, and found excellent agreement with their results.

Results and discussion

The non-dimensional governing eqs. (6), (7), (14), (22), and (23) subject to the respective boundary conditions (8), (15), and (24) are solved numerically using Runge-Kutta based shooting technique Sandeep and Sulochana [40]. Results depict the influence of the dimensionless physical governing parameters on the flow, heat and mass transfer in Casson and Williamson fluids. For numerical computations we considered the non-dimensional values as $A^*=B^*=0.1$, $\mathrm{Sc}=K_s=K=\delta=1$, $\mathrm{Pr}=2$, $M=\beta=0.5$. These values are kept as common in the entire study except the varied values are shown in respective figures and tables.

Figures 2-6 depict the effect of magneticfield on the flow velocity, temperature and concentration fields. It is evident that for higher values of magneticfield parameter we noticed fall in the velocity and homogeneous concentration field. An opposite results have been observed for temperature and heterogeneous field. This is due to the well-known fact that growth in the magneticfield develops the drag forces opposite to the flow. These forces produce the temperature near the surface. Due to this sense we had seen a raise in the temperature and depreciation in the velocity field. But due to the small variations in the temperature field we have noticed a mixed performance in the concentration profiles. It is evident to conclude that while compared with the Williamsons fluid, the momentum, concentration and temperature profiles of Casson fluid is highly influenced by the magneticfield parameter.

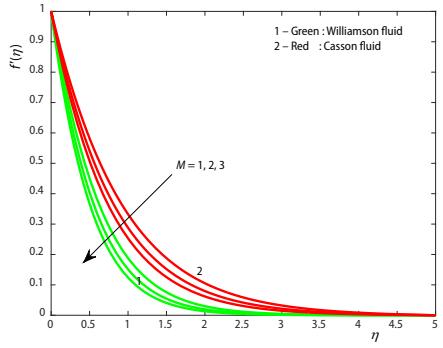

Figure 2. Velocity field for different values of magnetic parameter

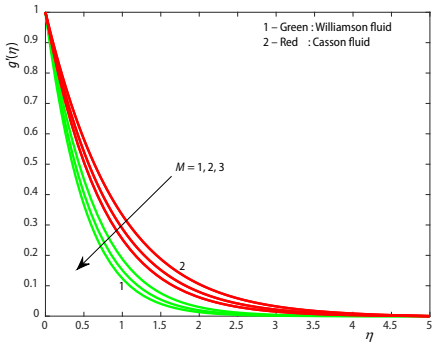

Figure 3. Velocity field for different values of magnetic parameter

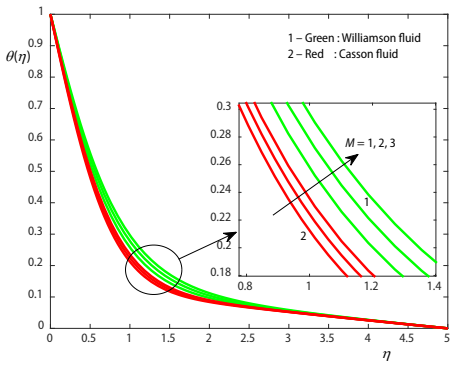

Figure 4. Temperature field for different values of magnetic parameter

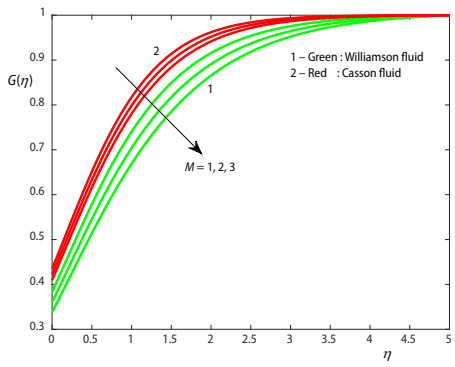

Figure 5. Concentration field for different values of magnetic parameter

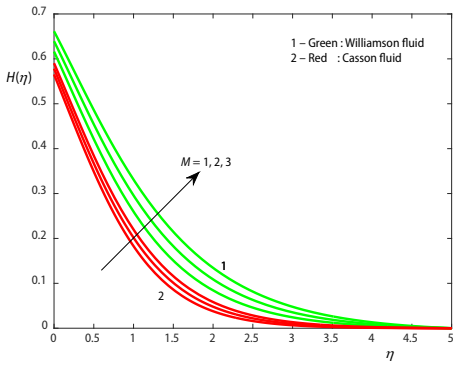

Figure 6. Concentration field for different values of magnetic parameter

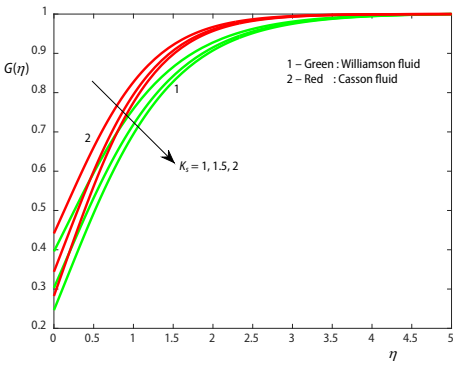

Figure 7. Concentration field for different values of heterogeneous parameter

Figsures 7 and 8 elucidates the effect of strength of heterogeneous parameter on concentration field. With an increment in the heterogeneous parameter we have perceived a fall in the homogeneous concentration profiles and a growth in the heterogeneous concentration field. It also observed that the influence of heterogeneous parameter is highly significant in Casson fluid. Because the concentration boundary-layer thickness of a Casson fluid is gradually

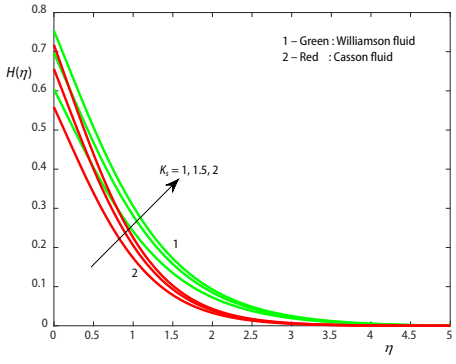

Figure 8. Concentration field for different values of heterogeneous parameter

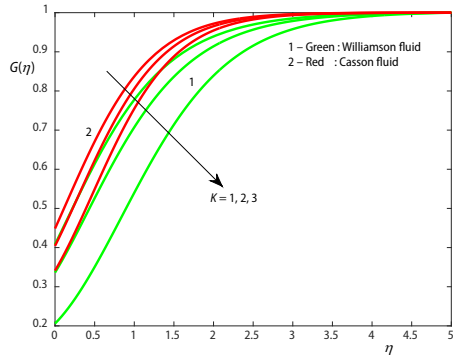

Figure 9. Concentration field for different values of homogeneous parameter

increases for smaller variations in the strength of heterogeneous parameter. Similar types of results have been observed with an increase in the strength of homogeneous parameter, these are displayed in figs. 9 and 10.

The influence of A^* and B^* on temperature field is displayed in figs. 11 and 12. It is evident that an increase in the space-dependent and temperature-dependent heat source/sink leads to enhance the temperature profiles throughout the boundary-layer. This agrees with the general fact that the positive values of A^* and B^* acts like heat generators. Generating the heat means releasing the heat energy to the flow, these causes to boost up the thermal boundary-layer thickness. It is interesting to note that the heat transfer production of the Casson fluid is comparatively better than the heat transfer production of the Williamsons fluid due to an increase in the non-uniform heat source/sink parameters.

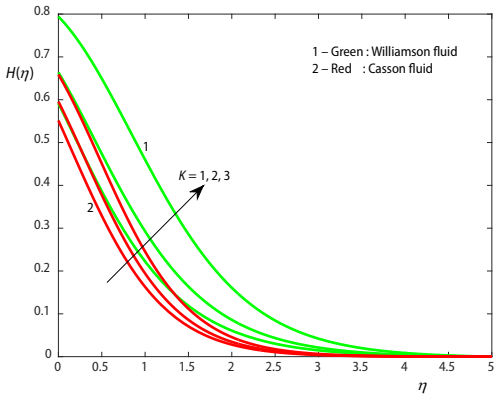

Figure 10. Concentration field for different values of homogeneous parameter

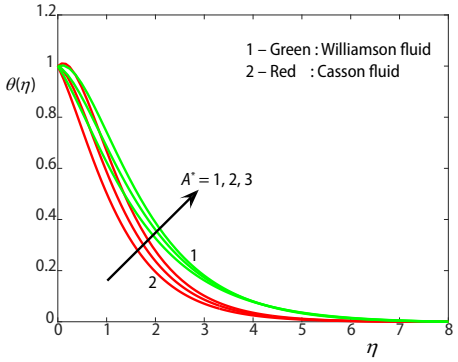

Figure 11. Temperature field for different values of non-uniform heat source/sink

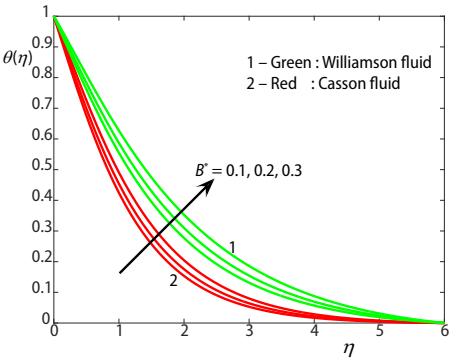

Figure 12. Temperature field for different values of non-uniform heat source/sink

Tables 1 depict the effects of non-dimensional principal parameters on skin-friction coefficients for axial and transverse directions for both Williamson and Casson fluids. It noticed that a rise in the values of magneticfield and porosity parameters reduces the friction factors for both Williamson and Casson fluids. An increase in homogeneous-heterogeneous reactions does not shown significant variation in the friction factors. Table 2 shows the variation in the local Nusselt number due to the change in governing physical parameters. It is clear that an increase in the magneticfield, porosity and non-uniform heat source/sink parameters reduces the heat transfer rate. Table 3 illustrates the effects of non-dimensional governing parameters on homogeneous-heterogeneous mass transfer rate. It is visible from that magnetic field parameter have tendency to enhances the homogeneous mass transfer rate and depreciates the heterogeneous mass transfer rate. We have seen a similar type of results with an increase in the homogeneous reaction parameter. But a raise in the heterogeneous parameter suppresses the mass transfer rate. Table 4 shows the validation of the present results with the existed literature. We found an excellent agreement of the present results with the published work.

Table 1. Variation in skin friction coefficients for different non-dimensional parameters

M	K_s	K	λ	Williamsons fluid		Casson fluid	
				$f''(0)$	$g''(0)$	$f''(0)$	$g''(0)$
1				–1.492849	–1.492849	–1.057005	–1.057005
2				–1.697492	–1.697492	–1.203730	–1.203730
3				–1.880330	–1.880330	–1.334684	–1.334684
	1			–1.379518	–1.379518	–0.975698	–0.975698
	1.5			–1.379518	–1.379518	–0.975698	–0.975698
	2			–1.379518	–1.379518	–0.975698	–0.975698
		1		–1.256455	–1.256455	–0.887428	–0.887428
		2		–1.256455	–1.256455	–0.887428	–0.887428
		3		–1.256455	–1.256455	–0.887428	–0.887428
			1	–1.379518	–1.379518	–0.975698	–0.975698
			2	–1.598379	–1.598379	–1.132687	–1.132687
			3	–1.791214	–1.791214	–1.270873	–1.270873

Table 2. Variation in local Nusselt number for different non-dimensional parameters

				Williamsons fluid	Casson fluid
M	A^*	B^*	λ	$-\theta'(0)$	$-\theta'(0)$
1				1.061980	1.168202
2				1.018127	1.138109
3				0.979309	1.111184
	1			1.112722	1.202743
	1.5			1.037060	1.122265
	2			0.961398	1.041787
		1		1.112722	1.202743
		2		0.932339	1.052899
		3		0.702747	0.878507
			1	1.086327	1.184807
			2	1.039332	1.152696
			3	0.998170	1.124307

Table 3. Variation in mass transfer rates for different non-dimensional parameters

			Williamsons	Fluid	Casson	Fluid
M	K_S	K	$-G'(0)$	$-H'(0)$	$-G'(0)$	$-H'(0)$
1			–0.383716	–0.616284	–0.434633	–0.565367
2			–0.360601	–0.639399	–0.421729	–0.578271
3			–0.338536	–0.661464	–0.409593	–0.590407
	1		–0.395795	-0.604205	–0.441462	–0.558538
	1.5		–0.454525	–0.696983	–0.515960	–0.656027
	2		–0.492470	–0.753765	–0.564671	–0.717664
		1	–0.408322	–0.591678	–0.448612	–0.551388
		2	–0.336087	–0.663913	–0.404352	–0.595648
		3	–0.205770	–0.794230	–0.341113	–0.658887

Table 4. Comparison of the values of $[1+(1/\beta)]f''(0)$ when $K = K_s = A^* = B^* = 0$

M	λ	β	Ahmad and Nazar [30]	Present results
0	0	∞	–1.0042	–1.00421
0	0	5	–1.0954	–1.09542
0	0.5	1	–1.7320	–1.73200
10	0	∞	–3.3165	–3.31653
10	0	5	–3.6331	–3.63311
10	0.5	1	–4.7958	–4.79582

Conclusions

The Casson fluid as well as Williamson fluids have specific importance in industrial as well as biomechanical engineering fields. The main motivation of this study due to importance of automatic system (Casson and Williamson fluids are small variation in viscosity) presented a numerical solution to analyze the heat and mass transfer production in MHD Casson and Williamson fluids past a stretching surface in the presence of non-uniform heat source/sink and homogeneous-heterogeneous reactions. We found that the heat and mass transfer production of Casson fluid is comparatively better than the heat and mass transfer production of Williamson fluid. Momentum boundary-layer thickness of Williamson fluid is effectively enhances due to variation in the non-dimensional parameters. The temperature profiles of the casson fluid are effectively enhances due to the external heat source. Homogeneous-heterogeneous parameters help to modulating the concentration boundary-layer thickness. This study can be useful in automatic manufacturing and designing processes based on the viscosity nature.

Acknowledgement

The authors extend Their appreciation to the Deanship of Scientific Research at King Saud University for funding this work through the research group project No RGP-080.

Nomenclature

A^*, B^* – non-uniform heat generation/absorption coefficient, [–]
a, b – concentration of the chemical species
c, d – constant parameters
Cf_x – skin friction coefficient in x-direction, [–]
Cf_y – skin friction coefficient in y-direction, [–]
c_p – specific heat capacity at constant pressure, [Jkg^{-1}K^{-1}]
D_A, D_B – diffusion coefficients
f, g – dimensionless velocities, [ms^{-1}]
G – strength of homogeneous concentration, [–]
H – strength of heterogeneous concentration, [–]
K – strength of homogeneous parameter, [–]
K_s – strength of heterogeneous parameter, [–]
k_c, k_s – rate constants
k_f – thermal conductivity, [Wm^{-1}K^{-1}]
M – magnetic field parameter, [–]
Nu_x – local Nusselt number, [–]
Pr – Prandtl number, [–]
q''' – non-uniform heat source/sink, [Ks^{-1}]
q_w – wall heat flux, [Wm^{-2}]
Re_x – local Reynolds number, [–]
Sc – Schmidt number, [–]
Sh_x – local Sherwood number, [–]
T – temperature of the fluid, [K]
T_w, T_∞ – temperatures of the near and far away from the surface
u, v – velocity components in x- and y-directions, respectively, [ms^{-1}]
u_w – velocity at the wall
x – distance along the surface, [m]
y – distance normal to the surface, [m]

Greek symbols

α_f – diffusion coefficient, [m^{2}s^{-1}]
β – Casson fluid parameter, [–]
Γ – relaxation time constant
δ – ratio of diffusion coefficient, [–]
η – similarity variable
θ – dimensionless temperature, [K]
λ – non-Newtonian fluid parameter, [–]
μ – dynamic viscosity of the fluid, [kgm^{-1}s^{-1}]

μ_∞ – viscosity of the ambient fluid
ν_f – kinematic viscosity, [m^2s^{-1}]
ρ – density of the fluid, [kgm^{-3}]
σ – electrical conductivity, [Sm^{-1}]
ϕ – nanoparticle volume fraction

Subscripts

f – fluid
w – condition at the wall
∞ – condition at the free stream

References

[1] Sakiadis, B. C., Boundary Layer Behavior on Continuous Solid Surface: Boundary Layer Equations for Two-Dimensional and Axisymmetric Flow, *J. Amer. Inst. Chem. Eng., 7* (1961), 1, pp. 26-28
[2] Ali, M. E., Al-Yousef, F., Laminar Mixed Convection from a Continuously Moving Vertical Surface with Suction or Injection, *Heat and Mass Transfer, 33* (1998), 4, pp. 301-306
[3] Magyari, E., *et al*., Heat and Mass Transfer Characteristics of the Self-Similar Boundary-Layer Flows Induced by Continuous Surfaces Stretched with Rapidly Decreasing Velocities, *Heat and Mass Transfer, 38* (2001), 1-2, pp. 65-74
[4] Chamkha, A. J., MHD Flow of a Uniformly Stretched Vertical Permeable Surface in the Presence of Heat Generation/Absorption and a Chemical Reaction, *Int. Comm. Heat Mass Trans., 30* (2003), 3, pp. 413-422
[5] Raptis, A., Perdikis, C., Viscous Flow over a Non-Linearly Stretching Sheet in the Presence of a Chemical Reaction and Magnetic Field, *Int. J. Non-Linear Mech*., *41* (2006), 4, pp. 527-529
[6] Patil, P. M., Kulkarni, P. S., Effects of Chemical Reaction on Free Convective Flow of a Polar Fluid through a Porous Medium in the Presence of Internal Heat Generation, *Int. J. Thermal Sci., 47* (2008), 8, pp. 1043-1054
[7] Ali, M. E., The Effect of Variable Viscosity on Mixed Convection Heat Transfer along a Vertical Moving Surface, *Int. J. of Thermal Science*, *45* (2006),1, pp. 60-69
[8] Cortell, R., MHD Flow and Mass Transfer of an Electrically Conducting Fluid of Second Grade in a Porous Medium over a Stretching Sheet with Chemically Reactive Species, *Chemical Engineering and Processing*, *46* (2007), 8, pp. 721-728
[9] Raju, C. S. K., *et al.,* Effects of Induced Magnetic Field and Homogeneous-Heterogeneous Reactions on Stagnation Flow of a Casson Fluid, *Engineering Science and Technology, an International Journal, 19* (2016), 2, pp. 875-887
[10] Haq, R. U., *et al*., Convective Heat Transfer and MHD Effects on Casson Nanofluid Flow over a Shrinking Sheet, *Cent. Eur. J. Phys*., *12* (2014), 12, pp. 862-871
[11] Hussain, A., *et al.*, Unsteady Boundary Layer Flow and Heat Transfer of a Casson Fluid Past an Oscillating Vertical Plate with Newtonian Heating, *Plos One, 9* (2014), Oct., e108763
[12] Raju, C. S. K., *et al*., Heat and Mass Transfer in Magneto Hydrodynamic Casson Fluid over an Exponentially Permeable Stretching Surface, *Eng. Sci. Tech., an Int. J.*, *19* (2016), 1, pp. 45-52
[13] Nadeem, S., *et al*., MHD Flow of a Casson Fluid over an Exponentially Shrinking Sheet, *Scientia Iranica B, 19* (2012), 6, pp. 1550-1553
[14] Nadeem, S., *et al*., MHD Three-Dimensional Casson Fluid Flow Past a Porous Linearly Stretching Sheet, *Alexandria Engineering J., 52* (2013), 4, pp. 577-582
[15] Ramzan, M., *et al*., MHD Three-Dimensional Flow of Couple Stress Fluid with Newtonian Heating, *Eur. Phys. J. Plus, 49* (2013), May, pp. 128
[16] Hayat, T., *et al*., Three-Dimensional Stretched Flow of Jeffrey Fluid with Variable Thermal Conductivity and Thermal Radiation, *Applied Mathematics and Mech*., *34* (2013), 7, pp. 823-832
[17] Ali, M. E., The Buoyancy Effects on the Boundary Layers Induced by Continuous Surfaces Stretched with Rapidly Decreasing Velocities, *Heat and Mass Transfer, 40* (2004), 3-4, pp. 285-291
[18] Mahantha, G., Shaw, S., 3-D Casson Fluid Flow Past a Porous Linearly Stretching Sheet with Convective Boundary Condition, *Alexandria Eng. J., 54* (2015), 3, pp. 653-659
[19] Sandeep, N., *et al*., Effects of Aligned Magnetic Field and Radiation on the Flow of Ferrofluids over a Flat Plate with Non-Uniform Heat Source/Sink, *Int. J. Sci. Eng., 8* (2015), 2, pp. 151-158
[20] Hayat, T., *et al*., Soret and Dufour Effects in the Flow of Williamson Fluid over an Unsteady Stretching Surface with Thermal Radiation, *Z. Naturforsch., 70* (2015), 4, pp. 235-243
[21] Khan, N. A., *et al*., Boundary Layer Flow of Williamson Fluid with Chemically Reactive Species Using Scaling Transformation and Homotopy Analysis Method, *Math. Sci. Lett*., *3* (2014), 3, pp. 199-205
[22] Hayat, T., *et al*., Heat and Mass Transfer Analysis on the Flow of a Second Grade Fluid in the Presence of Chemical Reaction, *Physics Letters A*, *372* (2008), 14, pp. 2400-2408

[23] Annimasun, I. L., *et al*., Unequal Diffusivities Case of Homogeneous-Heterogeneous Reactions Within Viscoelastic Fluid Flow in the Presence of Induced Magneticfield and Nonlinear Thermal Radiation, *Alexandria Engineering Journal*, *55* (2015), 2, pp. 1595-1606
[24] Hayat, T., *et al*., Homogeneous-Heterogeneous Reactions in Peristaltic Flow with Convective Conditions, *Plos One, 9* (2014), 12, e113851
[25] Bachok, N., *et al*., On the Stagnation Point Flow Towards a Stretching Sheet with Homogeneous-Heterogeneous Reactions Effects, *Commun. Nonlinear Sci. Numer. Simul., 16* (2011), 11, pp. 4296-4302
[26] Chatterjee, A., Heat Transfer Enhancement in Laminar Impinging Flows with a Non-Newtonian Inelastic Fluid, *J. Non Newtonian Fluid Mech*., *211* (2014), Sept., pp. 50-61
[27] Delenda, N., *et al*., Primary and Secondary Instabilities of Viscoelastic Mixutres Saturating a Porous Medium: Application to Separation of Species, *J. Non Newtonian Fluid Mech., 181-182* (2012), Aug., pp. 11-21
[28] Ramesh, G. K., *et al*., Heat Transfer in MHD Dusty Boundary Layer Flow of over an Inclined Stretching Surface with Non-Uniform Heat Source/Sink, *Advances in Mathematical Physics*, *2012* (2012) ID 657805
[29] Awais, M., et al., Hydromagnetic Couple-Stress Nanofluid Flow over a Moving Convective Wall: OHAM Analysis, *Acta Astronautica*, *129* (2016), Dec., pp. 271-276
[30] Ramesh, G. K., Numerical Study of the Influence of Heat Source on Stagnation Point Flow Towards a Stretching Surface of a Jeffrey Fluid Nanoliquid, *Journal of Engineering*, *2015* (2015), ID 382061
[31] Nadeem, S., Saleem, S., Analytical Study of Third Grade Fluid over a Rotating Vertical Cone in the Presence of Nanoparticles, *International Journal of Heat and Mass Transfer, 85* (2015), June, pp. 1041-1048
[32] Ramesh, G. K., *et al.,* MHD Mixed Convection Flow of a Viscoelastic Fluid over an Inclined Surface with a Nonuniform Heat Source/Sink, *Canadian Journal of Physics, 91* (2013), 12, pp. 1074-1080
[33] Salman, S., et al., Time-Dependent Second-Order Viscoelastic Fluid Flow on Rotating Cone with Heat Generation and Chemical Reaction, *Journal of Aerospace Engineering, 29* (2016), 4, 04016009
[34] Awais, M., *et al.,* Dual Solutions for Nonlinear Flow Using Lie Group Analysis, *PloS One*, *10* (2015), 11, e0142732
[35] Nadeem, S., *et al.,* The Effect of Variable Viscosities on Micro polar Flow of Two Nanofluids, *Zeitschrift für Naturforschung A, 71* (2016), 12, pp. 1121-1129
[36] Raju, C. S. K., Sandeep, N., Unsteady Three-Dimensional Flow of Casson-Carreau Fluids Past a Stretching Surface, *Alexandria Engineering Journal, 55* (2016), 2, pp. 1115-1126
[37] Nadeem, S., *et al.*, Flow of Williamson Fluid over a Stretching Sheet, *Brazilian Journal Chemical Engineering, 30* (2013), 3, pp. 619-625
[38] Chaudhary, M. A., Merkin, J. H., A Simple Isothermal Model for Homogeneous-Heterogeneous Reactions in Boundary Layer Flow: I. Equal Diffusivities, *Fluid Dynamics Res., 16* (1995), 6, pp. 311-333
[39] Ahmad, K., Nazar, R., Magnetohydrodynamic Three-Dimensional Flow and Heat Transfer over a Stretching Surface in a Viscoelastic Fluid, *J. Science and Technology, 3* (2011), 1, pp. 33-46
[40] Sandeep, N., Sulochana, C., Dual Solution for Unsteady Mixed Convection Flow of MHD Micropalar Fluid over a Stretching/Shrinking Sheet with Non-Uniform Heat Source/Sink, *Engineering Science and Technology, An International Journal*, *18* (2015), 4, pp. 1-8

Paper submitted: April 26, 2016
Paper revised: April 3, 2017
Paper accepted: April 5, 2017